

Dual-constrained Deep Semi-Supervised Coupled Factorization Network with Enriched Prior

Yan Zhang, Zhao Zhang, *Senior Member, IEEE*, Yang Wang, Zheng Zhang, Li Zhang, Shuicheng Yan, *Fellow, IEEE*, and Meng Wang, *Senior Member, IEEE*

Abstract—Nonnegative matrix factorization is usually powerful for learning the “shallow” parts-based representation, but it clearly fails to discover deep hierarchical information within both the basis and representation spaces. In this paper, we technically propose a new enriched prior based Dual-constrained Deep Semi-Supervised Coupled Factorization Network, called DS²CF-Net, for learning the hierarchical coupled representations. To extract hidden deep features, DS²CF-Net is modeled as a deep-structure and geometrical structure-constrained neural network. Specifically, DS²CF-Net designs a deep coupled factorization architecture using multi-layers of linear transformations, which coupled updates the bases and new representations in each layer. To improve the discriminating ability of learned deep representations and deep coefficients, our network clearly considers enriching the supervised prior by the joint deep coefficients-regularized label prediction, and incorporates enriched prior information as additional label and structure constraints. The label constraint can enable the samples of the same label to have the same coordinate in the new feature space, while the structure constraint forces the coefficient matrices in each layer to be block-diagonal so that the enhanced prior using the self-expressive label propagation are more accurate. Our network also integrates the adaptive dual-graph learning to retain the local manifold structures of both the data manifold and feature manifold by minimizing the reconstruction errors in each layer. Extensive experiments on several real databases demonstrate that our DS²CF-Net can obtain state-of-the-art performance for representation learning and clustering.

Keywords—Deep semi-supervised coupled factorization network; deep representation learning; dual label and structure constraints; enriched prior; clustering

I. INTRODUCTION

In emerging visual data analytics applications, one core topic is about how to learn a good and compact expression of complex high-dimensional real-world data by uncovering the explanatory factors hidden in the observed inputs. To learn effective representations, many methods can be adopted, among which Matrix Factorization (MF) is one of the widely-used techniques for representation learning [1-5][48-51]. Classical MF methods consist of Singular Value Decomposition (SVD) [2], Vector Quantization (VQ) [3], Nonnegative Matrix Factorization (NMF) [4] and

Concept Factorization (CF) [5], etc. It is noteworthy that NMF and CF use the nonnegative constraints on the factorization matrices, which enables them to learn parts-based representations that correspond to distinguishing features that are useful for subsequent clustering and classification [4-5]. NMF and CF aim at decomposing a data matrix X into two or three matrix factors whose product is the approximation to X [4-5], where one factor contains the basis vectors capturing high-level features and each sample is reconstructed by a linear combination of the bases. The other factor corresponds to the new compact representation.

Although CF offers an obvious advantage over NMF, that is, it can be performed in kernel space and any other representation space, they both cannot encode the local geometry of the features and also fail to use the label information even if available. First, to handle the locality preserving issue, some graph regularized methods have been proposed, such as Graph Regularized NMF (GNMF) [6], Graph-Regularized LCF (GRLCF) [8], Locally Consistent CF (LCCF) [7], Graph-Regularized CF with Local Coordinate (LGCF) [9], Dual Regularization NMF (DNMF) [12] and Dual-graph regularized CF (GCF) [13]. These algorithms usually use the graph Laplacian to smooth the representation and encode geometrical information of the data space. Different from GNMF and LCCF, both DNMF and GCF can not only capture the geometrical structures of data manifold but also the feature manifold by using the dual-graph regularized strategy [10-13]. Although the above algorithms have obtained encouraging clustering results by considering the local properties, they still suffer from some shortcomings: 1) High sensitivity and tricky optimal determination of the number k of nearest neighbors [14-15]; 2) Separating the graph construction from matrix factorization by two independent steps cannot ensure the pre-encoded weights to be optimal for the subsequent representation; 3) They cannot take advantage of label information to improve the representation and clustering due to the unsupervised nature, similarly as NMF and CF. Second, for the discriminative MF, some semi-supervised algorithms have been proposed, such as Constrained Nonnegative Matrix Factorization (CNMF) [16], Constrained Concept Factorization (CCF) [17] and Semi-supervised GNMF (SemiGNMF) [6]. SemiGNMF incorporates partial label information into the graph construction, while CNMF and CCF define the representations consistent with the known label information by defining an explicit label constraint matrix so that the original labeled samples sharing the same label can be mapped into the same class in a low-dimensional space. Although CNMF, SemiGNMF and CCF can use label information of labeled samples clearly, they still fail to fully utilize the unlabeled samples, since they did not consider predicting the labels of the unlabeled samples and mapping them into their respective subspaces in feature space as well by learning an explicit label indicator matrix for the unlabeled data. In addition, CNMF, SemiGNMF and CCF also cannot self-express the input data in a recovered feature subspace. It is noteworthy that retaining the local geometry

-
- Y. Zhang and L. Zhang are with the School of Computer Science and Technology, Soochow University, Suzhou, China. (e-mail: zhang-yan0712suda@gmail.com, zhangliml@suda.edu.cn)
 - Z. Zhang, Y. Wang and M. Wang are with the Key Laboratory of Knowledge Engineering with Big Data (Ministry of Education), Hefei University of Technology, Hefei, China. (e-mails: cszzhang@gmail.com, yeungwangresearch@gmail.com, eric.mengwang@gmail.com)
 - Z. Zhang is with Bio-Computing Research Center, Harbin Institute of Technology, Shenzhen, China, and is also with Pengcheng Laboratory, Shenzhen, China. (e-mail: darrenzz219@gmail.com)
 - S. Yan is with the YITU Technology, China; also with the Department of Electrical and Computer Engineering, National University of Singapore, Singapore 117583. (e-mail: shuicheng.yan@yitu-inc.com)

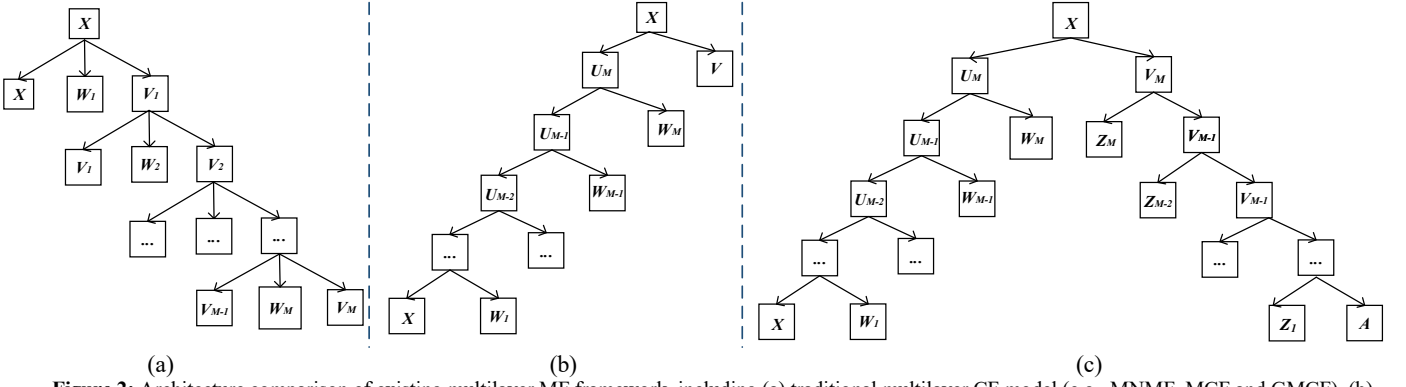


Figure 2: Architecture comparison of existing multilayer MF framework, including (a) traditional multilayer CF model (e.g., MNMF, MCF and GMCF), (b) optimized multilayer CF model (e.g., DSCF-Net), and (c) our proposed DS²CF-Net.

II. RELATED WORK

In this section, we introduce the related single-layer and multi-layer frameworks to our proposed DS²CF-Net.

A. Related Single-layer CF based Frameworks

We first show the closely-related single-layer CF and its variants.

Concept Factorization (CF) [5]. Given a nonnegative data matrix $X = [x_1, x_2, \dots, x_N] \in \mathbb{R}^{D \times N}$, where x_i is a sample vector, N is the number of samples and D is the original dimensionality. Denote by $U \in \mathbb{R}^{D \times r}$ and $V \in \mathbb{R}^{N \times r}$ two nonnegative matrix factors whose product $UV^T \in \mathbb{R}^{D \times N}$ is an approximation to X , where r is the rank. By representing each basis by a linear combination of x_i , i.e., $\sum_{i=1}^N w_{ij} x_i$, where $w_{ij} \geq 0$, CF proposes to solve the following minimization problem:

$$O = \|X - XWV^T\|_F^2, \quad s.t. \ W, V \geq 0, \quad (1)$$

where $W = [w_{ij}] \in \mathbb{R}^{N \times r}$, XW approximates the bases, V^T is the learned representation of X , which can be applied for clustering, and V^T is the transpose of the representation matrix V .

Self-Representative Manifold CF (SRMCF) [24]. SRMCF integrates the adaptive neighbor structure and manifold regularizer into the CF framework. Specifically, it considers WV^T in CF as the coefficient matrix based on the dictionary of the raw data matrix X . Then, it incorporates the self-representation with the adaptive neighbor structure to assign neighbors for all samples. The objective function of SRMCF is defined as

$$O = \|X - XWV^T\|_2^2 + \lambda_1 \sum_{i,j=1}^N \left\{ \left\| (WV^T)_i - (WV^T)_j \right\|_2^2 \Theta_{ij} + \xi \Theta_{ij}^2 \right\}, \quad (2)$$

$$+ \lambda_2 \text{tr}(V^T L^V V), \quad s.t. \ W \geq 0, V \geq 0, \forall i \ \Theta_i^T \mathbf{1} = 1, 0 \leq \Theta_i \leq 1$$

where $\mathbf{1}$ is an all-ones column vector, ξ is a positive trade-off parameter, and Θ_{ij} denotes the probability of $x_j \in [x_1, x_2, \dots, x_N]$ (excluding itself) being connected to x_i as a neighbor. $\Theta_i \in \mathbb{R}^{N \times 1}$ is a vector with the j -th element as Θ_{ij} . Note that the constraints $\Theta_i^T \mathbf{1} = 1$ and $0 \leq \Theta_i \leq 1$ are used to ensure the probability property of Θ_i . L^Θ is the Laplacian matrix of Θ and L^V is a predefined Laplacian matrix by 0-1 weight based on the Euclidean distances between each sample $x_j \in [x_1, x_2, \dots, x_N]$ as [47]. λ_1 and λ_2 are two parameters. Note that SRMCF still suffers from the tough choice of the number of nearest neighbors of each sample.

Dual-graph regularized CF (GCF) [13]. GCF introduces the graph regularizers of both data manifold and feature manifold into CF simultaneously by constructing a k nearest neighbor data graph G^V and a k nearest feature graph G^U . Then, GCF uses the 0-1 weighting scheme for G^V and G^U and defines the corresponding weight matrices S^V and S^U as follows:

$$(S^V)_{js} = \begin{cases} 1 & \text{if } x_s \in N_k(x_j), j, s = 1, 2, \dots, N \\ 0 & \text{otherwise} \end{cases}, \quad (3)$$

$$(S^U)_{js} = \begin{cases} 1 & \text{if } x_s^T \in N_k(x_j^T), j, s = 1, 2, \dots, M \\ 0 & \text{otherwise} \end{cases}$$

where $N_k(x_j)$ denotes the set of the k nearest neighbors of x_j . The graph Laplacian over G^V and G^U are defined as $L^V = D^V - S^V$ and $L^U = D^U - S^U$, where D^V and D^U are diagonal matrices with entries being $(D^V)_{jj} = \sum_s (S^V)_{js}$ and $(D^U)_{jj} = \sum_s (S^U)_{js}$. Finally, the objective function of GCF is formulated as

$$O = \|X - XWV^T\|_F^2 + \alpha \text{tr}(V^T L^V V) + \beta \text{tr}(W^T L^W W), \quad (4)$$

where $L^W = X^T L^U X$, α and β are parameters. Clearly, GCF has the difficulty issue to choose the optimal k on various datasets.

Constrained CF (CCF) [17]. To improve the discriminating power, CCF extends CF to the semi-supervised scenario by using label information of the labeled data as an additional constraint. Suppose that the data matrix X contains a labeled sample set $X_L \in \mathbb{R}^{D \times l}$ and an unlabeled set $X_U \in \mathbb{R}^{D \times u}$, that is, $l + u = N$ and $X = [X_L, X_U] \in \mathbb{R}^{D \times (l+u)}$, where l and u are the numbers of labeled and unlabeled samples respectively, then CCF guides the constrained CF by defining a label constraint matrix A . Denote by $A_L \in \mathbb{R}^{l \times c}$ the class indicator matrix defined on labeled data, where c is the number of classes. The element $(A_L)_{ij}$ is defined as 1 if x_i is labeled as the j -th class, and 0 otherwise. Since CCF did not define an explicit class indicator for X_U and simply used an identity matrix $I_{u \times u}$ of dimension $u \times u$ for unlabeled data. Thus, the overall label constraint matrix A is defined as

$$A = \begin{bmatrix} (A_L)_{l \times c} & 0 \\ 0 & I_{u \times u} \end{bmatrix} \in \mathbb{R}^{(l+u) \times (c+u)}. \quad (5)$$

To ensure the data points sharing the same label to be mapped into the same class in low-dimensional space (i.e., same v_i), CCF

imposes the label constraints by an auxiliary matrix Z :

$$V = AZ. \quad (6)$$

By substituting $V=AZ$ into CF, CCF finds a non-negative matrix $W \in \mathbb{R}^{N \times r}$ and a non-negative auxiliary matrix $Z \in \mathbb{R}^{(c+u) \times r}$ from the following objective function:

$$O = \|X - XWZ^T A^T\|_F^2, \text{ s.t. } W, Z \geq 0. \quad (7)$$

B. Related Deep/Multilayer MF Frameworks

We then introduce the architectures of several existing related deep/multilayer matrix factorization algorithms.

Traditional multilayer MF. The multilayer MF methods of this category usually use the output of the previous layer (i.e., intermediate representation V) as the input of subsequent layer directly, without properly considering to optimize the representation and basis vectors in each layer. Classical methods include MNMF, MCF and GMCF, etc. These methods aim to minimize the objective function in each layer independently and simply use V_{m-1} ($m \geq 2$) obtained in the $(m-1)$ -th layer as the input of the m -th layer. That is, they cannot ensure the intermediate representation to be a good representation for subsequent layers, which may cause the degraded performance. We show the multilayer structure of this category methods in Fig.2(a).

Optimized deep MF models. The recent fast developments of deep learning have led to a renewed interest in designing the deep or multi-layer MF [18-23][49-51] for deep representation learning and clustering. One of the most widely-used approach to extend the single-layer model to the deep model of M -layers is to iteratively take the outputted representation of the last layer as the inputs of the next layer directly for further MF [18-21], where M denotes the number of layers, such as Multilayer NMF (MNMF) [18], Multilayer CF (MCF) [19], Spectral Unmixing using Multilayer NMF (MLNMF) [20] and Graph regularized multilayer CF (GMCF) [21]. However, such a strategy may be invalid and even unreasonable in practice, because in this case the learned representation of the first layer determines the learning abilities of the whole framework, while most existing models cannot ensure this issue. In other words, one cannot ensure that the output of the last layer is already a good representation, so directly feeding it to the next layer may mislead and degrade the learning power of subsequent layers. To address these issues, the other popular and optimized way is to discover hidden deep feature information by adopting multiple layers of linear transformations and updating the basis vectors or feature representations in each layer [22-23], such as Weakly-supervised Deep MF (WDMF) [22], Deep Semi-NMF (DSNMF) [23] and Deep Self-representative Concept Factorization Network (DSCF-Net) [43]. In general, WDMF aims at fixing the basis vectors and optimizes the representations in each layer, while DSCF-Net argues that learning a set of optimal basis vectors will be more important and accurate for reconstructing given data by a linear combination of the bases, which aims at optimizing the basis vectors to update the representation matrix in each layer. It is noted that WDMF mainly focuses on the social image understanding tasks, i.e., tag refinement, tag assignment and image

retrieval, and the initial input of WDMF is the tagging matrix F rather than the data matrix X as other MF models. In addition, DSCF-Net also incorporates the subspace recovery process and adaptive locality-preserving power into a united framework for enhancing the feature representations. Different from WDMF and DSCF-Net, DSNMF is just a two-stage approach, where the strategy in the first stage is the same as traditional MNMF, MCF, MLNMF and GMCF, i.e., directly feeding the learned representation matrix of the last layer into the next layer for further MF, and the second stage refines the representation matrices and basis vectors directly based on the outputs of each layer in the first stage using an independent step. It is clear that the refining step can obtain deep features, but the learned deep features are directly based on the first stage. As such, DSNMF will also suffer from the same performance-degrading issue as those traditional MNMF, MCF, MLNMF and GMCF. Moreover, DSNMF also cannot preserve the manifold structures of samples, especially in an adaptive manner, and also ignores the supervised prior information for learning. Note that we illustrate the multilayer structure of DSCF-Net for uncovering the hidden feature representations in Fig.2(b). For comparison, we also show the deep coupled factorization network of DS²CF-Net in Fig.2(c), from which we see that DS²CF-Net jointly optimizes the basis vectors and representation matrix in each layer.

III. DEEP SEMI-SUPERVISED COUPLED FACTORIZATION NETWORK (DS²CF-Net)

In this section, we introduce the formulation of our DS²CF-Net. Given the partially labeled data matrix $X = [X_L, X_U] \in \mathbb{R}^{D \times (l+u)}$, where l and u are the numbers of labeled and unlabeled samples. The base model of DS²CF-Net is built based on the semi-supervised formulation of CCF, i.e., incorporating a label constraint matrix A and approximating the representation matrix V with AZ , where Z is an auxiliary matrix. However, to enhance the representation and clustering abilities, DS²CF-Net designs a hierarchical and coupled factorization framework that has M layers. Technically, our DS²CF-Net is modeled as the formulation of learning M updated pairs of representation matrices and basis vectors $XW_1 \dots W_M$, and M updated label constraint matrices A . That is, the label constraint matrix A is optimized and enriched for unlabeled data in our model, instead of fixing it as CCF.

A. Factorization Model

Before presenting the factorization model, we first describe the initial optimization problem of DS²CF-Net as follows:

$$O_{DS^2CF-Net} = \|X - XW_0 \dots W_M (Z_0 \dots Z_M)^T A^T\|_F^2 + \alpha J_2 + \beta J_3 + \gamma J_1, \quad (8)$$

s.t. $\forall_{i \in \{1, 2, \dots, M\}} W_i \geq 0, Z_i \geq 0$

where $XW_0 \dots W_M$ corresponds to the set of deep basis vectors, $(Z_0 \dots Z_M)^T A^T$ denotes the learned deep low-dimensional representation, $\|X - XW_0 \dots W_M (Z_0 \dots Z_M)^T A^T\|_F^2$ is called the deep reconstruction error, J_1 , J_2 and J_3 will be shown shortly. W_0 and Z_0 are added to facilitate the description and optimization, and both are fixed to be the identity matrices. Note that the overall label constraint matrix A in our network is defined as

$$A = \begin{bmatrix} A_L & 0 \\ 0 & A_U \end{bmatrix} \in \mathbb{R}^{(l \times u) \times (c+e)}, \quad A_L \in \mathbb{R}^{l \times c}, A_U \in \mathbb{R}^{u \times c}, \quad (9)$$

where A_L is the class indicator matrix for labeled data, which can be easily defined as [17], i.e., $(A_L)_{i,j} = 1$ if sample x_i is labeled as the class j , and else 0. Notably, DS²CF-Net also optimizes an explicit class indicator A_U for the unlabeled data to enrich the supervised prior rather than fixing it to be an identity matrix as CCF, which can well group the representation of both the labeled and unlabeled samples based on the enriched supervised prior based dual label and structure constraints.

According to the self-expressive properties on the coefficient matrix [24], the reconstruction error can be rewritten as

$$\|X - XR_M\|_F^2, \text{ where } R_M = W_0 \dots W_M (Z_0 \dots Z_M)^T A^T, \quad (10)$$

where R_M can be regarded as the meaningful coefficient matrix self-expressing X . Then, the proposed multi-layer factorization model can be presented as follows:

$$\begin{aligned} X &\leftarrow U_M V_M^T \\ U_M &= U_{M-1} W_M & V_M &= V_{M-1} Z_M \\ &\vdots & & \vdots \\ U_2 &= U_1 W_2 & V_2 &= V_1 Z_2 \\ U_1 &= X W_1 & V_1 &= A Z_1 \end{aligned} \quad \text{and} \quad (11)$$

where U_m ($m = 1, 2, \dots, M$) is the set of basis vectors of the m -th layer, V_m^T ($m = 1, 2, \dots, M$) is the low-dimensional representation, W_m ($m = 1, 2, \dots, M$) is the intermediate matrix for updating basis vectors and Z_m ($m = 1, 2, \dots, M$) is the intermediate auxiliary matrix for updating the representations. It is noteworthy that the factorization model of our DS²CF-Net does not need to initialize the network using traditional multi-layer model as DSNMF that initializes the network by directly feeding the learned representation matrix of the last layer into the next layer for MF, and the deep factorization of DSNMF completely depends on the outputs of the traditional multi-layer model.

B. Enriched Prior based Dual-constraints

We first show how to enrich supervised prior information. Specifically, DS²CF-Net learns a robust label predictor $P \in \mathbb{R}^{D \times c}$ over labeled data by minimizing a label fitness error $\|A_L - X_L^T P\|_F^2$, where c is the number of classes, which can map each sample x_i into a label space in terms of $P^T x_i$. In addition, DS²CF-Net also explores preserving neighborhood information of embedded soft labels $P^T X_i$ in the projective label space, which self-expresses it using the coefficient matrix R_M . As such, the formulation of learning the label predictor P can be defined as

$$\begin{aligned} J_1 &= \|A_L - X_L^T P\|_F^2 + \|P^T X - P^T X R_M\|_F^2 + \|P\|_{2,1} \\ &= \|A_L - X_L^T P\|_F^2 + \|P^T X - P^T X (W_0 \dots W_M (Z_0 \dots Z_M)^T A^T)\|_F^2 + \|P\|_{2,1} \end{aligned} \quad (12)$$

where $L_{2,1}$ -norm based regularization can enable the label predictor to be robust the outliers and error in data. In addition, the $L_{2,1}$ -norm can enable the discriminative labels to be predicted and estimated in the latent sparse feature subspace.

Enriched prior based label constraint. After the label predictor P is obtained, we can easily predict the soft label of each unlabeled sample $x_i \in X_U$ as $x_i^T P$. Then, we obtain A_U by using the normalized soft labels that are described as follows:

$$(A_U)_{ij} = (X_U^T P)_{ij} / \sum_{j=1}^c (X_U^T P)_{ij}. \quad (13)$$

That is, the normalized soft labels meet the column-sum-to-one constraint $A_U \mathbf{1} = \mathbf{1}$, where $\mathbf{1} \in \mathbb{R}^{c \times 1}$ is a column vector of ones. Note that one recent related work is called Robust Semi-Supervised Adaptive Concept Factorization (RS²ACF) [42] has also discussed the partially labeled CF model and considered learnt a class indicator A_U for unlabeled data, but our DS²CF-Net is different from it in three aspects. First, DS²CF-Net is a deep MF model, while our RS²ACF is a single-layer model. Second, the manifold smoothness for label prediction in DS²CF-Net is defined based on the self-expressive deep coefficient matrix in each layer, while RS²ACF encodes the manifold smoothness by learning an extra weight matrix and is performed in a single-layer mode. Third, DS²CF-Net defines the class indicator A_U based on the normalized soft labels of unlabeled data rather than directly embedding X_U into P . Since the predicted soft label value $(A_U)_{ij}$ indicates the probability of each x_i belonging to the class j , forcing $A_U \mathbf{1} = \mathbf{1}$ may be more accurate and reasonable.

Enriched prior based structure constraint. Since the coefficients $W_0 \dots W_M (Z_0 \dots Z_M)^T A^T$ can be used to characterize the locality of features, it ideally has a good block-diagonal structure, where each block corresponds to a subspace or a class. As such, each sample can be reconstructed more accurately by the samples of the same class as much as possible. Thus, we propose to introduce a block-diagonal structure constraint matrix Q to constrain the coefficient matrix by minimizing the approximation error between Q and $W_0 \dots W_M (Z_0 \dots Z_M)^T A^T$ in each layer:

$$J_2 = \|Q - W_0 \dots W_M (Z_0 \dots Z_M)^T A^T\|_F^2 + \|W_0 \dots W_M (Z_0 \dots Z_M)^T A^T\|_F^2, \quad (14)$$

where the structure constraint matrix Q is defined as follows:

$$Q = \begin{bmatrix} Q_L & 0 \\ 0 & Q_U \end{bmatrix} \in \mathbb{R}^{(l+u) \times (l+u)}, \quad Q_L = \begin{bmatrix} Q_1 & 0 & 0 & 0 \\ 0 & Q_2 & 0 & 0 \\ 0 & 0 & \dots & 0 \\ 0 & 0 & 0 & Q_c \end{bmatrix} \in \mathbb{R}^{l \times l}, \quad (15)$$

where Q_L and Q_U are the structure constraint matrices defined based on the labeled data X_L and unlabeled data X_U . Since the samples of X_L are originally labeled, Q_L is a strict block-diagonal matrix, where each block Q_i ($i = 1, 2, \dots, c$) is an $l_i \times l_i$ matrix of all ones, defined according to the labeled samples, and l_i is the number of samples in class i in X_L . For example, if we have 9 labeled samples, where x_1 and x_2 are from the class 1, x_3, x_4, x_5 and x_6 are from class 2 and the remaining ones are from class 3, the sub-matrices Q_1 , Q_2 and Q_3 can be defined as

$$Q_1 = \begin{bmatrix} 1 & 1 \\ 1 & 1 \end{bmatrix}, \quad Q_2 = \begin{bmatrix} 1 & 1 & 1 & 1 \\ 1 & 1 & 1 & 1 \\ 1 & 1 & 1 & 1 \end{bmatrix}, \quad Q_3 = \begin{bmatrix} 1 & 1 & 1 \\ 1 & 1 & 1 \\ 1 & 1 & 1 \end{bmatrix}.$$

It should be noted that we initiate Q_U by the cosine similarities over the samples in X_U and update Q_U in m -th ($m > 1$) layer using the cosine similarity matrix defined on the new representation of X_U , i.e., $(V_m)_{ij}, i \in \{l+1, \dots, N\}$. In this way, we can ensure the overall coefficient matrix $W_0 \dots W_M (Z_0 \dots Z_M)^T A^T$ to have a good structure for the representation learning.

C. Self-weighted Dual-graph Learning

To obtain the locality preserving representations, we further add the self-weighted dual-graph learning into DS²CF-Net, which can preserve the neighborhood information of both the deep basis vectors $XW_0 \dots W_M$ and representations $(Z_0 \dots Z_M)^T A^T$ in an adaptive manner at the same time. Specifically, we learn the data weight matrix $S^U \in \mathbb{R}^{N \times N}$ over the deep representations and the feature weight matrix $S^V \in \mathbb{R}^{D \times D}$ over the deep basis vectors adaptively by solving the following reconstructive loss:

$$J_3 = \left\| (XW_0 \dots W_M)^T - (XW_0 \dots W_M)^T S^U \right\|_F^2 + \left\| ((Z_0 \dots Z_M)^T A^T) - ((Z_0 \dots Z_M)^T A^T) S^V \right\|_F^2, \text{ s.t. } S^U \geq 0, S^V \geq 0 \quad (16)$$

Clearly, our DS²CF-Net defines the nonnegative dual-graph weights, which is different from that of GCF [13] in two aspects. First, GCF is a single-layer model that defines the weights over the “shallow” basis vectors and features, while our DS²CF-Net encodes the localities based on the deep basis vectors and features. Second, DS²CF-Net does not need to specify the number of nearest neighbors, suffered in GCF and the neighbors of each sample are determined automatically in DS²CF-Net by directly minimizing the reconstruction error. Moreover, the dual-graph weights are adaptively updated during the factorization process, which can enable our DS²CF-Net to be adaptive to different datasets and produce accurate feature representations.

D. Objective Function

Based on the above analysis, the final objective function of our DS²CF-Net method can be formulated as follows:

$$O_{DS^2CF-Net} = \min_{W_1, \dots, W_M, Z_1, \dots, Z_M, S^U, S^V, P} \left\| X - XW_0 \dots W_M (Z_1 \dots Z_M)^T A^T \right\|_F^2 + \alpha \left[\|Q - R_M\|_F^2 + \|R_M\|_F^2 \right] + \beta \left[\|U_M^T - U_M^T S^U\|_F^2 + \|V_M^T - V_M^T S^V\|_F^2 \right] + \gamma \left[\|A_L - X_L^T P\|_F^2 + \|P^T X - P^T X R_M\|_F^2 + \|P\|_{2,1} \right] \text{ s.t. } \forall_{m \in \{1, 2, \dots, M\}} W_m \geq 0, Z_m \geq 0, S^U \geq 0, S^V \geq 0 \quad (17)$$

where $U_M = XW_0 \dots W_M$, $V_M = A(Z_0 \dots Z_M)$ and $R_M = W_0 \dots W_M V_M^T$. Next, we describe the optimization procedures of DS²CF-Net.

IV. OPTIMIZATION

From the objective function of DS²CF-Net, we can easily find that the involved variables, i.e., W_m, Z_m ($m \in \{1, 2, \dots, M\}$), S^U, S^V , and P , depend on each other, so they cannot be solved directly. Following the common procedures, we present an iterative optimization strategy using the Multiplicative Update Rules (MUR) method [44-45] for obtaining local optimal solutions. Specifically, we solve the problem by updating the variables alternately

and optimize one of them each time by fixing the others. The detailed optimization procedures are shown as follows:

1) Fix others, update the factors W_m and Z_m :

We first show how to optimize the nonnegative matrices W_m and Z_m from the objective function. For the m -th layer, W_1, \dots, W_{m-1} , Z_1, \dots, Z_{m-1} and P are known and are all the constants, by defining $\Pi_{m-1} = W_0 \dots W_{m-1}$ and $\Lambda_{m-1} = Z_0 \dots Z_{m-1}$, the reduced sub-problem associated with W_m and Z_m can be defined as follows:

$$\min_{W_m, Z_m} \left\| X - X \Pi_{m-1} W_m (\Lambda_{m-1} Z_m)^T A^T \right\|_F^2 + \alpha \left(\|Q - R_M\|_F^2 + \|R_M\|_F^2 \right) + \beta \left(\|U_M^T - U_M^T S^U\|_F^2 + \|V_M^T - V_M^T S^V\|_F^2 \right) + \gamma \|P^T X - P^T X R_M\|, \text{ s.t. } W_m \geq 0 \quad (18)$$

where $U_M = X \Pi_{m-1} W_m$, $V_M = A \Lambda_{m-1} Z_m$ and $R_M = \Pi_{m-1} W_m (\Lambda_{m-1} Z_m)^T A^T$. Let ψ_{ik}^w and ψ_{ik}^z be the Lagrange multipliers for the constraints $(W_m)_{ik} \geq 0$ and $(Z_m)_{ik} \geq 0$, $\Psi_w = [\psi_{ik}^w]$ and $\Psi_z = [\psi_{ik}^z]$, then the Lagrange function can be constructed as

$$\begin{aligned} \wp = & \left\| X - X \Pi_{m-1} W_m (\Lambda_{m-1} Z_m)^T A^T \right\|_F^2 \\ & + \alpha \left[\|Q - \Pi_{m-1} W_m (\Lambda_{m-1} Z_m)^T A^T\|_F^2 + \|\Pi_{m-1} W_m (\Lambda_{m-1} Z_m)^T A^T\|_F^2 \right] \\ & + \beta \text{tr} \left[(X \Pi_{m-1} W_m)^T H_u (X \Pi_{m-1} W_m) + (A \Lambda_{m-1} Z_m)^T H_v (A \Lambda_{m-1} Z_m) \right] \\ & + \gamma \|P^T X - P^T X \Pi_{m-1} W_m (\Lambda_{m-1} Z_m)^T A^T\| + \text{tr}(\Psi_w W_m^T) + \text{tr}(\Psi_z Z_m^T) \end{aligned} \quad (19)$$

where $H_u = (I - S^U)(I - S^U)^T$, $H_v = (I - S^V)(I - S^V)^T$ and I denotes an identity matrix. Then, W_m and Z_m can be alternately updated by fixing others. Let $K_X = X^T X$, $K_A = A^T A$ and $K_P = X^T P P^T X$, the derivatives w.r.t. W_m and Z_m can be obtained as

$$\begin{aligned} \partial \wp / \partial W_m = & 2 \left(\Pi_{m-1}^T K_X \Pi_{m-1} W_m V_M^T V_M - \Pi_{m-1}^T K_X V_M \right) \\ & + 2\alpha \left(-\Pi_{m-1}^T Q V_M + 2Q^T \Pi_{m-1} W_m V_M^T V_M \right) \\ & + \beta \left(\Pi_{m-1}^T X^T (H_u + H_u^T) X \Pi_{m-1} W_m \right) \\ & + 2\gamma \left(\Pi_{m-1}^T K_P \Pi_{m-1} W_m V_M^T V_M - \Pi_{m-1}^T K_P V_M \right) + \Psi_w \end{aligned} \quad (20)$$

$$\begin{aligned} \partial \wp / \partial Z_m = & 2 \left(\Lambda_{m-1}^T K_A \Lambda_{m-1} Z_m U_M^T U_M - \Lambda_{m-1}^T K_A U_M \right) \\ & + 2\alpha \left(2\Lambda_{m-1}^T K_A \Lambda_{m-1} Z_m W_m^T Q^T \Pi_m - \Lambda_{m-1}^T A^T Q^T \Pi_m \right) \\ & + \beta \left(\Lambda_{m-1}^T (H_v + H_v^T) \Lambda_{m-1} Z_m K_A^T \right) \\ & + 2\gamma \left(\Lambda_{m-1}^T K_A \Lambda_{m-1} Z_m U_M^T P P^T U_M^T - \Lambda_{m-1}^T A^T K_P \Pi_m \right) + \Psi_z \end{aligned} \quad (21)$$

where $\Pi_m = \Pi_{m-1} W_m$, and Π_m is known when updating Z_m . By using the KKT conditions $\psi_{ik}^w (W_m)_{ik} = 0$ and $\psi_{ik}^z (Z_m)_{ik} = 0$, we can obtain the updating rules for W_m and Z_m :

$$(W_m)_{ik} \leftarrow (W_m)_{ik} \frac{(2\Pi_{m-1}^T K_X V_M + 2\alpha \Pi_{m-1}^T Q V_M + \Omega_w)_{ik}}{(2\Pi_{m-1}^T K_X \Pi_{m-1} W_m V_M^T V_M + \Phi_w)_{ik}}, \quad (22)$$

$$(Z_m)_{ik} \leftarrow (Z_m)_{ik} \frac{(2\Lambda_{m-1}^T A^T K_X \Pi_m + 2\alpha \Lambda_{m-1}^T A^T Q^T \Pi_m + \Omega_z)_{ik}}{(2\Lambda_{m-1}^T K_A \Lambda_{m-1} Z_m U_M^T U_M + \Phi_z)_{ik}}, \quad (23)$$

Algorithm 1: Optimization procedures of DS²CF-Net

Inputs: Partially labeled data matrix $X=[X_L, X_U]$, constant r and tunable model parameters α, β, γ .

Initialization: Initialize W and Z to be the random matrices; Initialize the label predictor P and label constraint matrix A using the labeled data; Initialize Q_U by the cosine similarities over X_U ; Initialize S^U using the cosine similarities over X and initialize S^V using the semi-supervised weights, i.e., supervised ones for X_L and the cosine similarities for X_U ; $t=0$.

For each fixed number m of layers:

While not converged do

1. Update the matrix factors W_m^{t+1} and Z_m^{t+1} by Eqs.(22-23), and then we can obtain $V_m^{t+1} = AZ_0 \dots Z_m^{t+1}$;
2. Update the weights $(S^U)^{t+1}$ and $(S^V)^{t+1}$ by Eqs.(25-26);
3. Update the linear label predictor P^{t+1} by Eq.(28), update the soft labels of X_U as $X_U^T P^{t+1}$, and then update A_U by Eq.(13);
4. Update the full label-constraint matrix A by Eq.(9);
5. Update Q_U by the cosine similarities defined based on $(V_m^{t+1})_i$, $i \in \{1, \dots, N\}$, and then update structure-constraint matrix Q ;
5. Check the convergence conditions: suppose $\|W_m^{t+1} - W_m^t\|_F^2 \leq \varepsilon$ and $\|V_m^{t+1} - V_m^t\|_F^2 \leq \varepsilon$, stop; else $t=t+1$.

End while

End for

Output: Learned optimal deep feature representation V_m^* .

where $\Phi_W = 4\alpha Q^T \Pi_{m-1} W_m V_M^T V_M + \beta \Pi_{m-1}^T X^T (H_u + H_u^T) X \Pi_{m-1} W + 2\gamma \Pi_{m-1}^T K_P \Pi_{m-1} W_m V_M^T V_M$, $\Phi_Z = 4\alpha \Lambda_{m-1}^T K_A \Lambda_{m-1} Z_m W_m^T Q^T \Pi_m + \beta \Lambda_{m-1}^T (H_v + H_v^T) \Lambda_{m-1} Z_m K_A^T + 2\gamma \Lambda_{m-1}^T K_A \Lambda_{m-1} Z_m U_M^T P P^T U_M$, $\Omega_W = 2\gamma \Pi_{m-1}^T K_P V_M$ and $\Omega_Z = 2\gamma \Lambda_{m-1}^T A^T K_P \Pi_m$ are auxiliary matrices.

2) Fix others, update the weight matrices S^U and S^V :

When other variables are computed, we can use them to update the dual-graph weights S^U and S^V by removing the irrelevant terms to S^U and S^V from the objective function. Let g_{ik}^u and g_{ik}^v denote the Lagrange multipliers for the constraints $S_{ik}^U \geq 0$ and $S_{ik}^V \geq 0$, $\Omega_u = [g_{ik}^u]$ and $\Omega_v = [g_{ik}^v]$, then the Lagrange function of the reduced problem can be similarly defined as

$$\hat{\phi} = \beta \left(\|U_M^T - U_M^T S^U\|_F^2 + \|V_M^T - V_M^T S^V\|_F^2 \right) + tr(\Omega_u S^{U^T}) + tr(\Omega_v S^{V^T}), \quad (24)$$

where $U_M = X \Pi_{m-1} W_m$ and $V_M = A \Lambda_{m-1} Z_m$ are known variables in this step. Based on the KKT conditions $g_{ik}^u S_{ik}^U = 0$ and $g_{ik}^v S_{ik}^V = 0$, we can obtain the updating rules for S^U and S^V :

$$(S^U)_{ik} \leftarrow (S^U)_{ik} \frac{((X \Pi_{m-1} W_m)(X \Pi_{m-1} W_m)^T)_{ik}}{((X \Pi_{m-1} W_m)(X \Pi_{m-1} W_m)^T S^U)_{ik}}, \quad (25)$$

$$(S^V)_{ik} \leftarrow (S^V)_{ik} \frac{((A \Lambda_{m-1} Z_m)(A \Lambda_{m-1} Z_m)^T)_{ik}}{((A \Lambda_{m-1} Z_m)(A \Lambda_{m-1} Z_m)^T S^V)_{ik}}. \quad (26)$$

3) Fix others, update the robust label predictor P :

Finally, we solve the projection P from Eq.(17), with W_m , Z_m , S^U and S^V known. By the properties of $L_{2,1}$ -norm [38-41], we have $\|P\|_{2,1} = 2tr(P^T B P)$, where B is a $D \times D$ diagonal matrix with entries $b_i = 1/(2\|p^i\|_2)$, where p^i is the i -th row of P . Thus, we can infer the label predictor P from the following problem:

$$\min_{P, B} \|A_L - X_L^T P\|_F^2 + \|P^T X (I - R_M)\|_F^2 + tr(P^T B P), \quad (27)$$

where each $p_i \neq 0$. By seeking the derivative of the above problem w.r.t. P , we can infer P in each layer as follows:

$$P = (X_L X_L^T + X H_M X^T + B)^{-1} X_L A_L, \quad (28)$$

where $H_M = (I - R_M)(I - R_M)^T$. After P is obtained, we can use it to update the diagonal matrix B and predict the labels of unlabeled samples. After that, we can use the normalized soft labels to optimize the label constraint matrix A for representation.

For complete presentation, we summarize the optimization procedures of DS²CF-Net in Algorithm 1, where the diagonal matrix B is initialized as an identity matrix. We initialize the linear label predictor $P = (X_L X_L^T + I)^{-1} X_L A_L$ as [42] and predict the soft labels of unlabeled data as $X_U^T P$, and then we normalize the soft labels by Eq.(13). Based on the normalized soft labels of unlabeled data, we can initialize the label constraint matrix A . Since DS²CF-Net jointly optimizes the set of basis vectors and representation matrices that are the major variables, to ensure the proposed algorithm to converge, the stopping condition can be simply set to $\|W_m^{t+1} - W_m^t\|_F^2 \leq \varepsilon$ and $\|V_m^{t+1} - V_m^t\|_F^2 \leq \varepsilon$ ($\varepsilon = 10^{-3}$) in the m -th layer, where $V_m^{t+1} = AZ_0 \dots Z_m^{t+1}$ is the computed representation matrix in the m -th layer and the approximation errors measure the difference between two sequential sets of basis vectors and representation matrices, which can make sure that the representation learning result will not change drastically.

A. Convergence Analysis

We present the convergence analysis of our DS²CF-Net in this section. Specifically, we can have the following theorem (i.e., Theorem 1) regarding the iterative updating rules of DS²CF-Net. Theorem 1 can ensure the convergence of the iterations and thus the final solution will be a local optimum.

Theorem 1: The objective function of our DS²CF-Net method in Eq.(17) is non-increasing based on the updating rules of Eqs. (22-23), (25-26) and (28). The objective function O of DS²CF-Net is invariant under these updating rules if and only if W_m , Z_m , S^U , S^V and P are at stationary points.

To prove Theorem 1, we adopt a similar convergence analysis method as CCF [17] and RS²ACF [42] by involving an auxiliary function to assist the analysis. We first show the definition of the auxiliary function and its properties.

Definition 1: $G(x, x')$ is an auxiliary function for $F(x)$ if the following conditions are satisfied:

$$G(x, x') \leq F(x), \quad G(x, x) = F(x). \quad (29)$$

Lemma 1: If G denotes an auxiliary function, then F is non-increasing under the following update:

$$x^{t+1} = \arg \min_x G(x, x'). \quad (30)$$

Proof: $F(x^{t+1}) \leq G(x^{t+1}, x^t) \leq G(x^t, x^t) = F(x^t)$.

Note that the equality $F(x^{t+1}) = F(x^t)$ holds only if x^t is a local minimum of $G(x, x^t)$. By iterating the above rules, we can

easily obtain a sequence of estimates that can converge to a local minimum $x_{\min} = \arg\min_x F(x)$. Next, we define an auxiliary function for our objective function and use **Lemma 1** to show that the minimum of the objective function is exactly our update rule, and therefore the **Theorem 1** can be proved.

We first prove the convergence of the updating rule in Eq.(22). For any entry $(W_m)_{ik}$ in W , let $F_{(W_m)_{ik}}$ be the part of objective function relevant to $(W_m)_{ik}$, i.e., Eq.(18). Since the update is essentially element-wise, it will be sufficient to show that each $F_{(W_m)_{ik}}$ is non-increasing under the updating rules. To prove it, we can define the auxiliary function G for $F_{(W_m)_{ik}}$.

Lemma 2: The following function is an auxiliary function for $F_{(W_m)_{ik}}$, which is only relevant to $(W_m)_{ik}$:

$$G(W_m, (W_m)_{ik}) = F_{(W_m)_{ik}}(W_m)_{ik} + F'_{(W_m)_{ik}}(W_m - (W_m)_{ik})^t + \frac{(2\Pi_{m-1}^T K_X \Pi_{m-1} W_m V_M^T V_M + \Phi_W)_{ik} (W_m - (W_m)_{ik})^t}{(W_m)_{ik}}^2. \quad (31)$$

Proof: The Taylor series expansion of $F_{(W_m)_{ik}}$ is described as

$$F_{(W_m)_{ik}}(W_m) = F_{(W_m)_{ik}}(W_m)_{ik} + F'_{(W_m)_{ik}}(W_m)_{ik}^t (W_m - (W_m)_{ik})^t + 1/2 F''_{(W_m)_{ik}}(W_m - (W_m)_{ik})^t. \quad (32)$$

Let $\tilde{\Pi}_{m-1} = \Pi_{m-1}^T (K_X + \gamma K_P) \Pi_{m-1}$ and $\hat{\Pi}_{m-1} = \Pi_{m-1}^T X^T (H_u + H_u^T) X \Pi_{m-1}$, we have

$$\partial^2 O_{DS^2CF-Net} / \partial (W_m)^2 = 2\tilde{\Pi}_{m-1} V_M^T V_M + 4\alpha \Pi_{m-1}^T Q V_M^T V_M + \beta \hat{\Pi}_{m-1}, \quad (33)$$

$$F''_{(W_m)_{ik}} = 2(\tilde{\Pi}_{m-1})_{ii} (V_M^T V_M)_{kk} + 4\alpha (\Pi_{m-1}^T Q)_{ii} (V_M^T V_M)_{kk} + \beta (\hat{\Pi}_{m-1})_{ii}. \quad (34)$$

$$\begin{aligned} (2\Pi_{m-1}^T K_X \Pi_{m-1} W_m V_M^T V_M + \Phi_W)_{ik} &= \sum_j 2(\tilde{\Pi}_{m-1})_{ij} (W_m)_{jk} (V_M^T V_M)_{kk} \\ &+ 4\alpha \sum_j (Q^T \Pi_{m-1})_{ij} (W_m)_{jk} (V_M^T V_M)_{kk} + \beta \sum_j (\hat{\Pi}_{m-1})_{ii} (W_m)_{ik} \\ &\geq 2(\tilde{\Pi}_{m-1})_{ii} (W_m)_{ik} (V_M^T V_M)_{kk} + 4\alpha (Q^T \Pi_{m-1})_{ii} (W_m)_{ik} (V_M^T V_M)_{kk} \\ &+ \beta (\hat{\Pi}_{m-1})_{ii} (W_m)_{ik} \\ &\geq (W_m)_{ik} \left[2(\tilde{\Pi}_{m-1})_{ii} (V_M^T V_M)_{kk} + 4\alpha (Q^T \Pi_{m-1})_{ii} (V_M^T V_M)_{kk} + \beta (\hat{\Pi}_{m-1})_{ii} \right] \\ &\geq (W_m)_{ik} \frac{1}{2} F''_{(W_m)_{ik}} \end{aligned} \quad (35)$$

Thus, we can easily conclude that $G(W_m, (W_m)_{ik}) \geq F_{(W_m)_{ik}}(W_m)$. Note that the auxiliary function for the objective function with regard to variable S^U is defined as follows:

Lemma 3: The following function $G(S^U, (S^U)_{ik})$, where

$$G(S^U, (S^U)_{ik}) = F_{(S^U)_{ik}}(S^U)_{ik} + F'_{(S^U)_{ik}}(S^U - (S^U)_{ik})^t + \frac{((X \Pi_{m-1} W_m)(X \Pi_{m-1} W_m)^T S^U)_{ik} (S^U - (S^U)_{ik})^t}{(S^U)_{ik}}^2, \quad (36)$$

is an auxiliary function for $F_{(S^U)_{ik}}$, which is part of the objective function that is only relevant to the variable $(S^U)_{ik}$.

Proof: The proof is essentially similar to that of **Lemma 2**. By comparing $G(S^U, (S^U)_{ik})$ with the Taylor series expansion of $F_{(S^U)_{ik}}$, we need to prove $((X \Pi_{m-1} W_m)(X \Pi_{m-1} W_m)^T S^U)_{ik} \geq (S^U)_{ik}^t F'_{(S^U)_{ik}}/2$. Since we have $\partial^2 O / \partial (S^U)^2 = 2((X \Pi_{m-1} W_m)(X \Pi_{m-1} W_m)^T)_{ii}$, $F'_{(S^U)_{ik}} = ((X \Pi_{m-1} W_m)(X \Pi_{m-1} W_m)^T)_{ii}$, and $((X \Pi_{m-1} W_m)(X \Pi_{m-1} W_m)^T S^U)_{ik} = \sum_j ((X \Pi_{m-1} W_m)(X \Pi_{m-1} W_m)^T)_{ij} (S^U)_{jk}$, $\geq (S^U)_{ik}^t ((X \Pi_{m-1} W_m)(X \Pi_{m-1} W_m)^T)_{ii} \geq \frac{1}{2} (S^U)_{ik}^t F'_{(S^U)_{ik}}$. (37)

As such, we can conclude that $G(S^U, (S^U)_{ik}) \geq F_{(S^U)_{ik}}(S^U)$.

Note that we can similarly prove that $G(Z_m, (Z_m)_{ik}) \geq F_{(Z_m)_{ik}}(Z_m)$, $G(P, P_{ik}^t) \geq F_{(P)_{ik}}(P)$, and $G(S^V, (S^V)_{ik}) \geq F_{(S^V)_{ik}}(S^V)$. Replacing $G(W_m, (W_m)_{ik})$, $G(Z_m, (Z_m)_{ik})$, $G(S^U, (S^U)_{ik})$, $G(P, P_{ik}^t)$, and $G(S^V, (S^V)_{ik})$ by Eq.(30), we can obtain the updating rules which are exactly the same updates as in Eqs.(22-23) (25-26) and (28) respectively. Thus, the objective function of our DS²CF-Net in Eq.(17) is non-increasing under the updates, which will be verified by the quantitative convergence analysis.

V. EXPERIMENTAL RESULTS AND ANALYSIS

In this section, we mainly conduct simulations to examine the data representation and clustering performance of our DS²CF-Net. The experimental results of DS²CF-Net are compared with 5 deep ML models (i.e., MNMF [18], MCF [19], GMCF [21], DSNMF [23] and DSCF-Net [43]), 3 single-layer MF models (i.e., DNMF [12], GCF [13] and SRMCF [24]), and four semi-supervised MF models (i.e., SemiGNMF [6], CNMF [16], CCF [17] and RS²ACF [42]). SemiGNMF adds class information of labeled data into the graph structures by modifying the graph weight matrix [6][17]. In this study, 6 public databases are involved, including two face image databases (i.e., AR [25] and MIT CBCL [26]), two object image databases (i.e., COIL100 [27] and ETH80 [28]), one handwritten dataset (i.e., USPS [29]), and one fashion products database (i.e., Fashion MNIST [46]). Some sample images of evaluated datasets are shown in Fig.3, and the detailed information of these databases is shown in Table 1, where we show the total number of samples, dimension and number of classes. For each face or object image, we follow the common procedures [30-31] to resize it into 32×32 pixels, forming a 1024-dimensional sample vector. Finally, we can obtain a data matrix with the vectorized representations of all the images as columns. The vectorized process for USPS and Fashion MNIST databases are similar. In this work, we normalize each column of the input data matrix to have unit norm for each database. We perform all experiments on a PC with Intel Core i5-4590 CPU @ 3.30 GHz 8G.

A. Visual Image Analysis by Visualization

Visualization of the adaptive weight matrix S^V . Since the low-dimensional representation $V_M = A(Z_0 \dots Z_M)$ is the final output of our DS²CF-Net, we first evaluate the representation ability of

Table 1: List of evaluated databases and database information.

Data Type	Name	#sample	#class	#dim
Face images	AR [25]	2600	100	1024
	MIT CBCL [26]	3240	10	1024
Object images	COIL100 [27]	7200	100	1024
	ETH80 [28]	3280	80	1024
Handwritten digits	USPS [29]	9298	10	256
Fashion products	Fashion MNIST [46]	70000	10	784

V_M by visualizing the reconstructed adaptive weights S^V on V_M . The AR face database is used and we randomly choose 2 categories to construct the adjacency graph S^V for clear observation, with 10 labeled images per class (that is, 20 labeled samples and 32 unlabeled samples in total). The weight matrix S^V is visualized in Fig.4, where we show the adaptive weights obtained by DS²CF-Net in the first four layers. Note that, the green box contains the weights on labeled data and the yellow box contains those on unlabeled data. We see that the constructed weight matrices have approximate block-diagonal structures in each layer. Specifically, the structures of the adaptive weights get clearer with less noise and inter-class connections as the number of layers increases, which means that the learned new representation

V_M has a strong representation ability and moreover our deep model can potentially improve the similarity measure.

Visualization of the structure constraint matrix Q . Since the structure constraint matrix Q determines the structures of the self-expressive coefficient matrix to encode the smoothness of manifolds in the process of label propagation, we also visualize its structures for observation. COIL100 database is used and we randomly choose 4 categories for the test, with 28 labeled samples per category (i.e., 28 labeled and 44 unlabeled). The structure constraint matrix Q is shown in Fig.5, where we show the results obtained in the first four layers, the green box and the yellow box contains the parts Q_L and Q_U on the labeled and unlabeled data, respectively. Q_L is defined according to the known labels, while Q_U is the cosine similarity defined based on the new representation of unlabeled samples. We find that the constraint matrix Q has a clear block-diagonal structure, and moreover the structures become better with the increasing number of layers, which implies that the structure constraint matrix Q in each layer has a strong discriminative representation power.

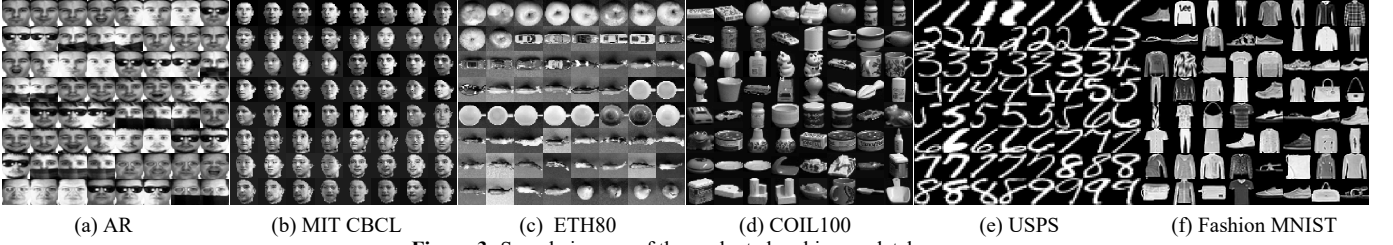


Figure 3: Sample images of the evaluated real image databases.

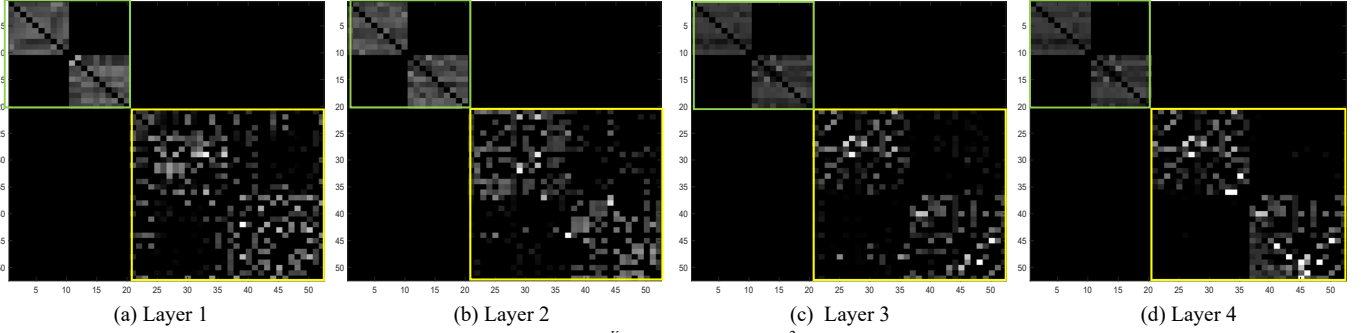


Figure 4: Visualization of the data weight matrix S^V obtained by our DS²CF-Net in the first four layers based on AR.

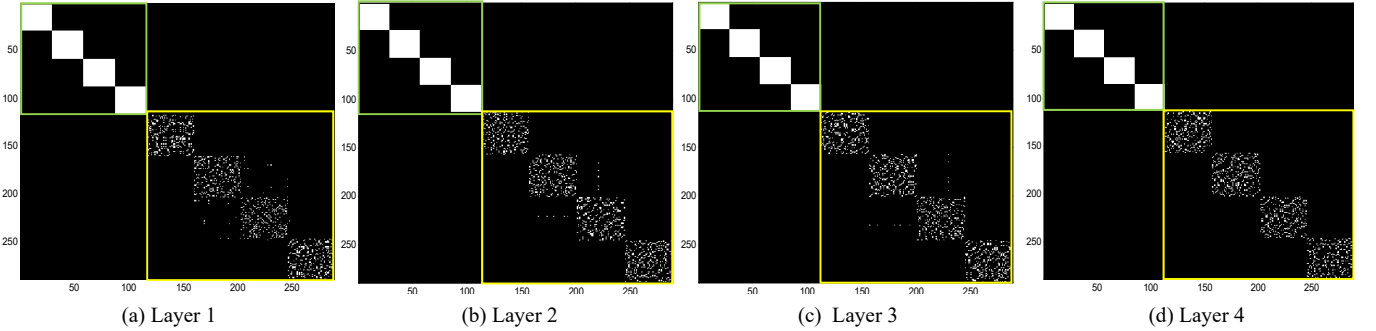


Figure 5: Visualization of the structure constraint matrix Q obtained by our DS²CF-Net in the first four layers based on COIL100.

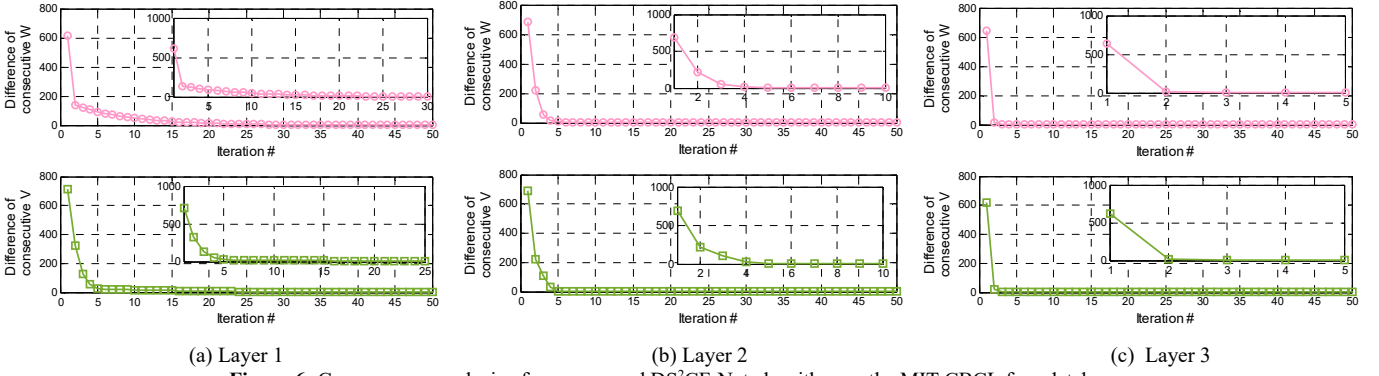


Figure 6: Convergence analysis of our proposed DS²CF-Net algorithm on the MIT CBCL face database.

B. Convergence Analysis

The involved variables of our DS²CF-Net are optimized alternately in each layer, we present some convergence analysis results using the MIT CBCL face database. Note that we use full MIT CBCL database with 40% samples labeled to train our method in this study. We present the convergence results of our DS²CF-Net in the first three layers in Fig.6, where the X-axis shows the number of iterations and Y-axis denotes the value of the difference between two consecutive sets of basis vectors (i.e., W^{t+1} and W^t) and two consecutive representations (i.e., V^{t+1} and V^t), respectively, i.e., $\|W^{t+1} - W^t\|_F^2$ and $\|V^{t+1} - V^t\|_F^2$. We see that: 1) our DS²CF-Net converges rapidly in each layer; 2) with the increasing number of layers, our model converges more rapidly due to the effects of deep structure, which usually converges within 5 iterations in the 3rd layer.

C. Quantitative Clustering Evaluation

(1) Clustering evaluation process. For the quantitative clustering evaluations, we perform the K-means algorithm with cosine distance on the representation obtained by each model. Following the procedures in [17][34], for each number K of clusters, we choose K categories from each database randomly and use the samples of K categories to form the data matrix X . The value of K is tuned from 2 to 6 in our study. The rank of the representation is set to K+1 for clustering as [17]. The clustering results are averaged based on 10 random selections of the K categories. For fair comparison, we choose 40% labeled samples per class for semi-supervised methods (i.e., SemiGNMF, CNMF, CCF, RS²ACF and our DS²CF-Net), and we set the number of layers to 3 for all compared multi-layer methods (i.e., MNMF, MCF, GMCF, DSNMF, DSCF-Net and our DS²CF-Net).

(2) Clustering evaluation metric. We employ two widely-used evaluation methods, i.e., *Accuracy* (AC) and *F-measure* [35-36]. AC is the percentage of the cluster labels to the true labels provided by the original data corpus, defined as follows:

$$AC = \left[\sum_{i=1}^N \delta(r_i, \text{map}(p_i)) \right] / N, \quad (38)$$

where N is the number of samples, and the function $\text{map}(p_i)$ is the permutation mapping function that maps the cluster label p_i obtained by the clustering method to the true label r_i provided by the data corpus, and the best mapping solution can be obtained by the Kuhn-Munkres algorithm [37] according to [35].

The clustering F-measure is defined as follows:

$$F_\mu = \frac{(\mu^2 + 1) \text{PRECISION} \times \text{RECALL}}{\mu^2 \text{PRECISION} + \text{RECALL}}, \quad (39)$$

where we set the parameter $\mu = 1$. Note that both values of the AC and F-measure range from 0 to 1, i.e., the higher the value is, the better the clustering result will be.

(3) Clustering evaluation results

Face Clustering. We first use face images to evaluate the clustering ability of learned representation by each method. AR and MIT CBCL face databases are evaluated. The clustering performance in terms of AC and F-measure over varied K numbers is tested. The clustering curves on the AR and MIT CBCL databases are shown in Fig.7 and Fig.8, respectively. The averaged AC and F-scores according to the curves in Fig.7 and Fig.8 are summarized in Tables 2-3, respectively. We can see that: (1) the obtained AC and F-measure of each method go down as the number of categories is increased, which is easy to understand, since clustering data of fewer categories is relatively easier than clustering more categories; (2) our DS²CF-Net delivers higher values of AC and F-measure than other compared methods in the investigated cases. Both RS²ACF and DSCF-Net performs better than other remaining methods in most cases. CNMF also delivers promising results over the MIT CBCL database.

Object Clustering. We then evaluate each method for representing and clustering the object image data. In this experiment, COIL100 and ETH80 object databases are evaluated. The clustering curves on ETH80 and COIL100 databases are shown in Fig.9 and Fig.10, respectively. The averaged AC and F-scores according to the curves in Fig.9 and Fig.10 are summarized in Tables 2-3, respectively. We can see that the increasing number of selected categories clearly decreases the performance of each method due to the fact that clustering data of fewer categories is relatively easier. It can also be found that DS²CF-Net delivers higher values of AC and F-measure than other evaluated methods in most cases. In addition, the semi-supervised SemiGNMF, CNMF, CCF and RS²ACF and methods can perform better than other algorithms using partially labelled data, where RS²ACF is the best method in this case. DSCF-Net also delivers relatively better clustering performance than other multilayer methods.

Handwritten Digit Clustering. We also examine the performance of each method for clustering handwritten digits of the

USPS database. In this study, we train each model based on the first 3000 samples of the database. The clustering curves under different numbers of selected categories of USPS database are shown in Fig.11 and Tables 2-3 describe the averaged AC and F-scores according to the curves in Fig.11. Similar observations can be found from the results. That is, the AC and F-measure of each algorithm go down as the number of categories increases. It can also be found that SemiGNMF, CNMF and RS²ACF deliver promising clustering results by using partially labeled data. Among the multilayer MF models, DSCF-Net obtains relatively better clustering performance than other methods. By further enriching the supervised prior by predicting the labels of unlabeled data, and designing a more reasonable dual-constrained deep structure, our DS²CF-Net outperforms all its competitors by delivering enhanced clustering performance.

Fashion Products Clustering. Finally, we test each method for representing the fashion product images of Fashion MNIST

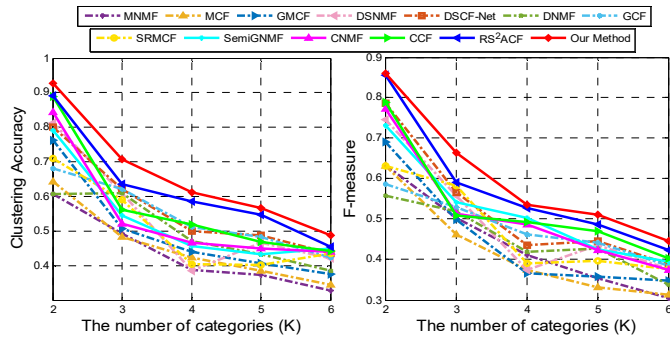


Figure 7: Clustering performance over varied K values on AR.

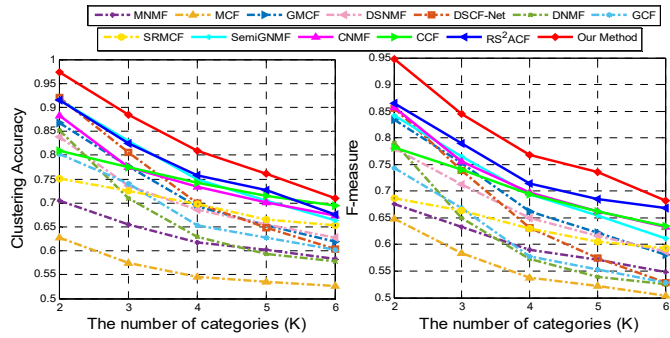


Figure 9: Clustering performance over varied K values on ETH80.

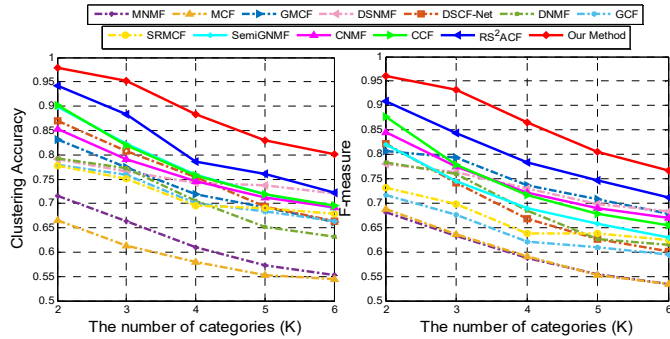


Figure 10: Clustering performance over varied K values on COIL100.

database. We train each model by a subset of Fashion MNIST, i.e., totally 10,000 samples from 10 classes. The clustering results in terms of AC and F-measure are evaluated and shown in Fig.12. Tables 2-3 describe the statistics in terms of averaged AC and F-scores according to Fig.12. From the results, we can similarly see that: 1) our DS²CF-Net delivers enhanced performance than other competitors in most cases, especially when the number of K is relatively small. We also find that semi-supervised methods can generally deliver enhanced performance than unsupervised ones. But note that SRMCF also obtains the promising results, which implies that the self-expression property is also important to improve the representation ability. It should be noted that our DS²CF-Net also employs the self-expression scheme in the proposed multilayer structures. In addition, one can also find that the results of the multilayer MNMF, MCF and GMCF models are worse than those of the single-layer models, which verifies that their multilayer structures of

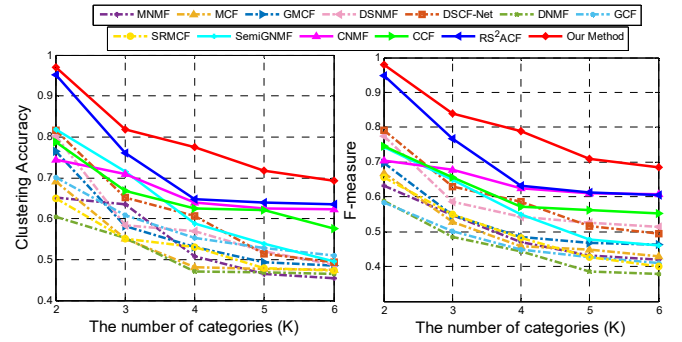


Figure 8: Clustering performance over varied K values on MIT CBCL.

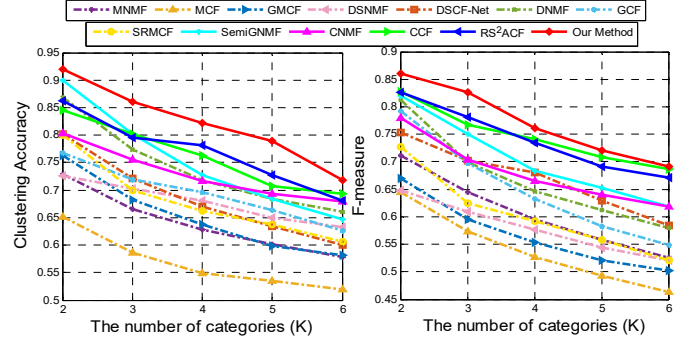


Figure 11: Clustering performance over varied K values on USPS.

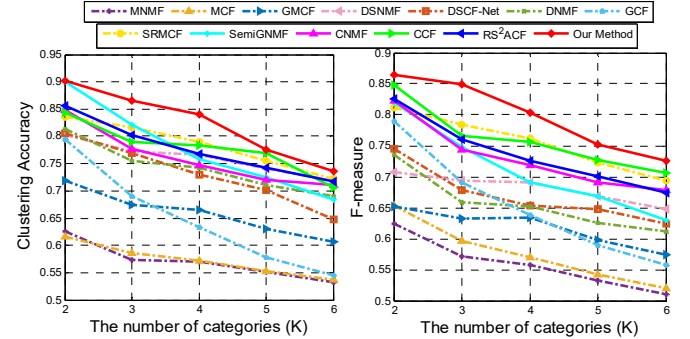


Figure 12: Clustering performance over varied K values on Fashion MNIST.

Table 2: Averaged clustering accuracies (AC) of the algorithms based on the evaluated six real mage databases.

Methods	AR	MIT CBCL	ETH80	COIL100	USPS	Fashion MNIST
	Mean \pm std	Mean \pm std	Mean \pm std	Mean \pm std	Mean \pm std	Mean \pm std
MNMF	0.4372 \pm 0.1121	0.5432 \pm 0.0942	0.6326 \pm 0.0481	0.6233 \pm 0.0670	0.6406 \pm 0.0592	0.5701 \pm 0.0348
MCF	0.4557 \pm 0.1166	0.5347 \pm 0.0932	0.5616 \pm 0.0410	0.5909 \pm 0.0492	0.5682 \pm 0.0525	0.5727 \pm 0.0302
GMCF	0.4985 \pm 0.1559	0.5714 \pm 0.1144	0.7217 \pm 0.1003	0.7358 \pm 0.0671	0.6524 \pm 0.0729	0.6590 \pm 0.0428
DSNMF	0.5383 \pm 0.1748	0.5926 \pm 0.1232	0.7088 \pm 0.0831	0.7519 \pm 0.0269	0.6786 \pm 0.0379	0.7601 \pm 0.0314
DSCF-Net	0.5688 \pm 0.1466	0.6168 \pm 0.1288	0.7353 \pm 0.1278	0.7579 \pm 0.0836	0.6853 \pm 0.0792	0.7307 \pm 0.0609
DNMF	0.5006 \pm 0.1022	0.5130 \pm 0.0636	0.6731 \pm 0.1123	0.7110 \pm 0.0709	0.7410 \pm 0.0830	0.7426 \pm 0.0472
GCF	0.5441 \pm 0.1050	0.5799 \pm 0.0775	0.6849 \pm 0.0837	0.7175 \pm 0.0502	0.6949 \pm 0.0540	0.6484 \pm 0.0986
SRMCF	0.5079 \pm 0.1368	0.5366 \pm 0.0710	0.6989 \pm 0.0408	0.7187 \pm 0.0432	0.6811 \pm 0.0746	0.7841 \pm 0.0460
SemiGNMF	0.5347 \pm 0.1492	0.6315 \pm 0.1332	0.7725 \pm 0.1006	0.7782 \pm 0.0838	0.7520 \pm 0.1010	0.7779 \pm 0.0847
CNMF	0.5443 \pm 0.1701	0.6685 \pm 0.0554	0.7529 \pm 0.0816	0.7589 \pm 0.0644	0.7293 \pm 0.0503	0.7605 \pm 0.0551
CCF	0.5763 \pm 0.1801	0.6552 \pm 0.0810	0.7468 \pm 0.0460	0.7787 \pm 0.0839	0.7621 \pm 0.0642	0.7782 \pm 0.0492
RS ² ACF	0.6226 \pm 0.1647	0.7271 \pm 0.1363	0.7800 \pm 0.0930	0.8189 \pm 0.0909	0.7697 \pm 0.0690	0.7775 \pm 0.0545
Our method	0.6595\pm0.1690	0.7944\pm0.1096	0.8276\pm0.1041	0.8887\pm0.0764	0.8219\pm0.0757	0.8236\pm0.0676

Table 3: Averaged F-score values of the algorithms based on the evaluated six real mage databases.

Methods	AR	MIT CBCL	ETH80	COIL100	USPS	Fashion MNIST
	Mean \pm std	Mean \pm std	Mean \pm std	Mean \pm std	Mean \pm std	Mean \pm std
MNMF	0.4414 \pm 0.1302	0.4999 \pm 0.0884	0.6035 \pm 0.0506	0.5980 \pm 0.0602	0.6070 \pm 0.0735	0.5592 \pm 0.0433
MCF	0.4228 \pm 0.1303	0.5060 \pm 0.0984	0.5593 \pm 0.0579	0.6004 \pm 0.0625	0.5400 \pm 0.0712	0.5765 \pm 0.0517
GMCF	0.4524 \pm 0.1462	0.5321 \pm 0.0982	0.6902 \pm 0.1029	0.7448 \pm 0.0549	0.5683 \pm 0.0665	0.6180 \pm 0.0311
DSNMF	0.4985 \pm 0.1576	0.5888 \pm 0.1077	0.6694 \pm 0.0780	0.7308 \pm 0.0416	0.5799 \pm 0.0506	0.6817 \pm 0.0236
DSCF-Net	0.5241 \pm 0.1605	0.6035 \pm 0.1183	0.6655 \pm 0.1317	0.6920 \pm 0.0901	0.6700 \pm 0.0654	0.6696 \pm 0.0463
DNMF	0.4522 \pm 0.0875	0.4563 \pm 0.0868	0.6156 \pm 0.1090	0.6940 \pm 0.0759	0.6695 \pm 0.0908	0.6569 \pm 0.0476
GCF	0.4811 \pm 0.0782	0.4741 \pm 0.0707	0.6144 \pm 0.0897	0.6434 \pm 0.0508	0.6503 \pm 0.0972	0.6531 \pm 0.0914
SRMCF	0.4751 \pm 0.1216	0.5031 \pm 0.1031	0.6356 \pm 0.0389	0.6657 \pm 0.0465	0.6040 \pm 0.0785	0.7551 \pm 0.0470
SemiGNMF	0.5192 \pm 0.1323	0.5756 \pm 0.1189	0.7135 \pm 0.0915	0.7087 \pm 0.0758	0.7050 \pm 0.0805	0.7117 \pm 0.0741
CNMF	0.5139 \pm 0.1543	0.6457 \pm 0.0435	0.7213 \pm 0.0887	0.7407 \pm 0.0708	0.6814 \pm 0.0636	0.7308 \pm 0.0575
CCF	0.5327 \pm 0.1484	0.6170 \pm 0.0821	0.7028 \pm 0.0592	0.7408 \pm 0.0894	0.7461 \pm 0.0553	0.7607 \pm 0.0539
RS ² ACF	0.5770 \pm 0.1678	0.7132 \pm 0.1469	0.7447 \pm 0.0818	0.7984 \pm 0.0783	0.7412 \pm 0.0637	0.7373 \pm 0.0590
Our method	0.6038\pm0.1642	0.8001\pm0.1181	0.7956\pm0.1033	0.8663\pm0.0819	0.7722\pm0.0708	0.7991\pm0.0600

directly feeding the learned representation from the last layer to the next layer is indeed not reasonable.

D. Ablation Study

(1) Clustering with different proportions of label data. We first evaluate each semi-supervised matrix factorization models, i.e., CNMF, CCF, SemiGNMF, RS²ACF and our DS²CF-Net, by using different numbers of labeled data in each class. In this study, for each database the proportion of labeled samples varies from 10% to 90%, and we randomly choose three categories for this test. We average the results over 10 random selections of categories and 30 initialization for the K-means clustering for each MF approach to avoid the randomness. The clustering results based on the evaluated databases are reported in Fig.13. We see that: (1) the increasing number of labeled samples can greatly improve the clustering performance of each method. It can also be found that the improvement by our DS²CF-Net over other compared methods is more obvious, especially when the proportion of label data is relatively small; (2) our DS²CF-Net delivers better results across different labeled proportions by fully mining the intrinsic relations between the labeled and unlabeled data, and predicting the labels of unlabeled samples to enrich the supervised prior knowledge. RS²ACF also performs well by delivering better results than other remaining methods.

(2) Clustering with different numbers of layers. We explore the effects of the number of layers on the representation learning and clustering abilities of each multilayer model, including MNMF, MCF, GMCF, DSNMF, DSCF-Net and our DS²CF-

Net. In this simulation, we vary the number of layers from 1 to 10 with step 1. For each database, we randomly choose 3 categories for the clustering evaluations. The averaged clustering ACs are illustrated in Fig.14, from which we see that: 1) our DS²CF-Net delivers the highest accuracies than other methods in most cases; 2) the increase of the number of layers can generally improve the clustering results, which implies that discovering hidden deep features can indeed improve the performance. However, the clustering results of MNMF, DSNMF, MCF and GMCF go down apparently when the number of layers passes 4 in most cases, which maybe because MNMF, MCF and GMCF cannot ensure the intermediate representation from the previous layer to be a good representation for subsequent layers. Note that the first stage of DSNMF is performed similarly as MNMF, MCF and GMCF, thus it also suffers from the degrading issue as the number of layers is increased to a high level. This observation can once again show that the multilayer structures of directly feeding the learned representation from the last layer to the next layer are not reasonable. By updating the basis vectors to optimize the low-dimensional representation in each layer, DSCF-Net also perform well by delivering higher and more stable results than other remaining methods, i.e., MNMF, DSNMF, MCF and GMCF. By this analysis, we can choose a proper number of layers for each multilayer MF model for the representation and clustering tasks in the experiments.

(3) Parameter sensitivity analysis in the objective function. Finally, we investigate the effects of model parameters on the

representation learning ability of our DS²CF-Net that has three trade-off parameters, i.e., α , β and γ . Because the optimal parameter selection is still an open issue, we use the widely-used grid search and linear strategy [32-33] in our experiments to select the most important parameters. Specifically, we firstly fix $\gamma=1$ to tune α and β from the candidate set $\{10^{-5}, 10^{-4}, \dots, 10^5\}$. Then, we use the selected α and β to tune γ over each database. We randomly choose the samples of three categories to train our model, the number of layers is set to three and the pro-

portion of labeled data is set to 40% for each database. The results are averaged based on 5 random initializations of the cluster centers for the K-means clustering algorithm. The parameter selection results are shown in Fig.15. We see that our method can obtain better clustering results when α is set to around 10^{-1} and β is set to a relatively small value around 10^{-4} for different datasets, which is a good phenomenon for the parameter selection. Note that we summarize the best choice of the model parameters of our DS²CF-Net algorithm in Table 4.

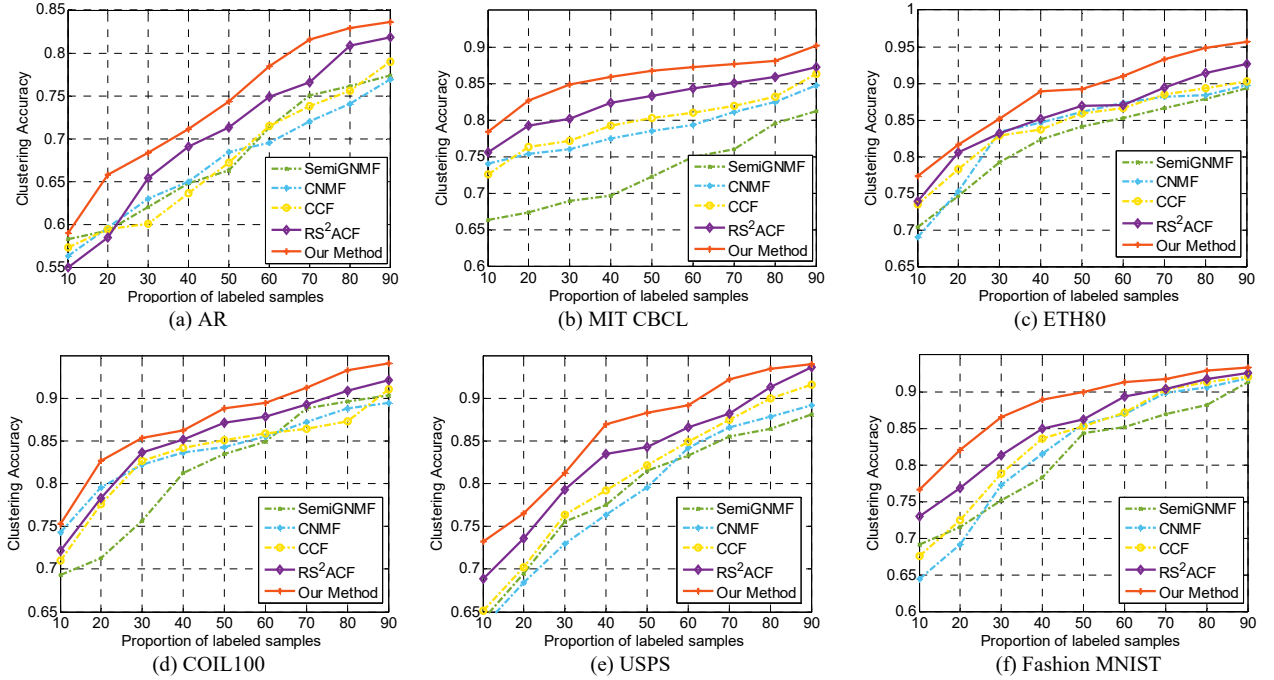


Figure 13: Clustering accuracies vs. varied proportions of labeled samples over the evaluated image databases.

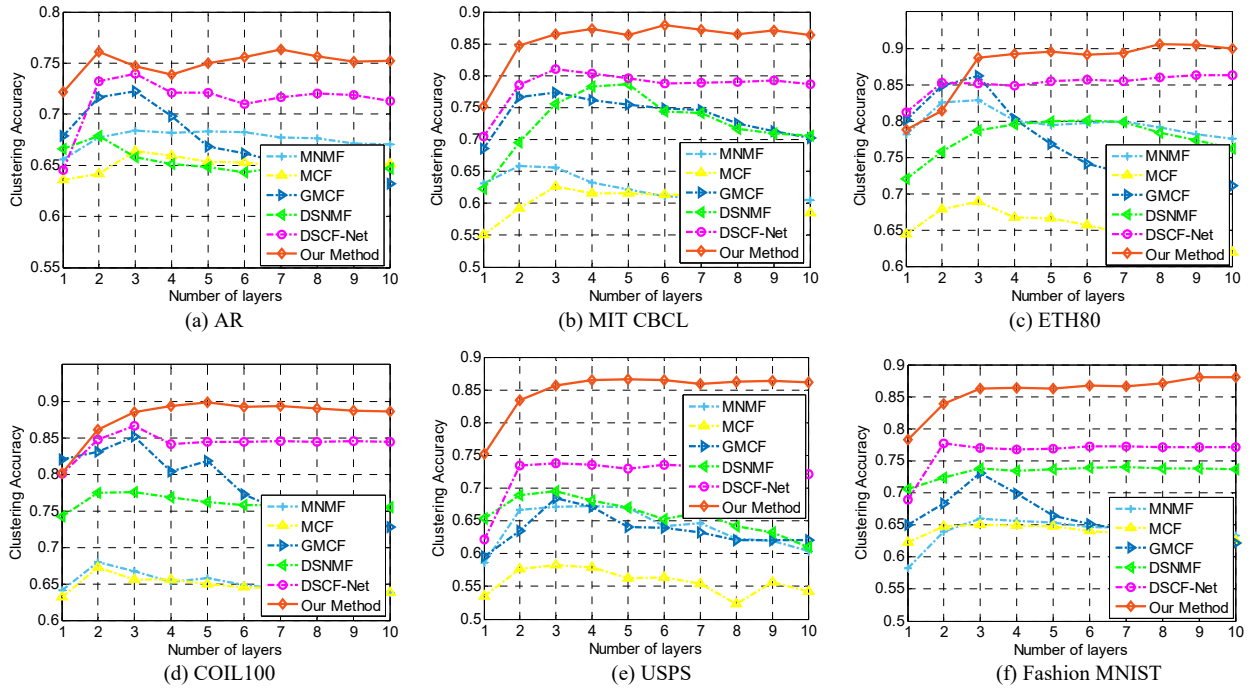


Figure 14: Clustering accuracies vs. varied number of layers based on the evaluated image databases.

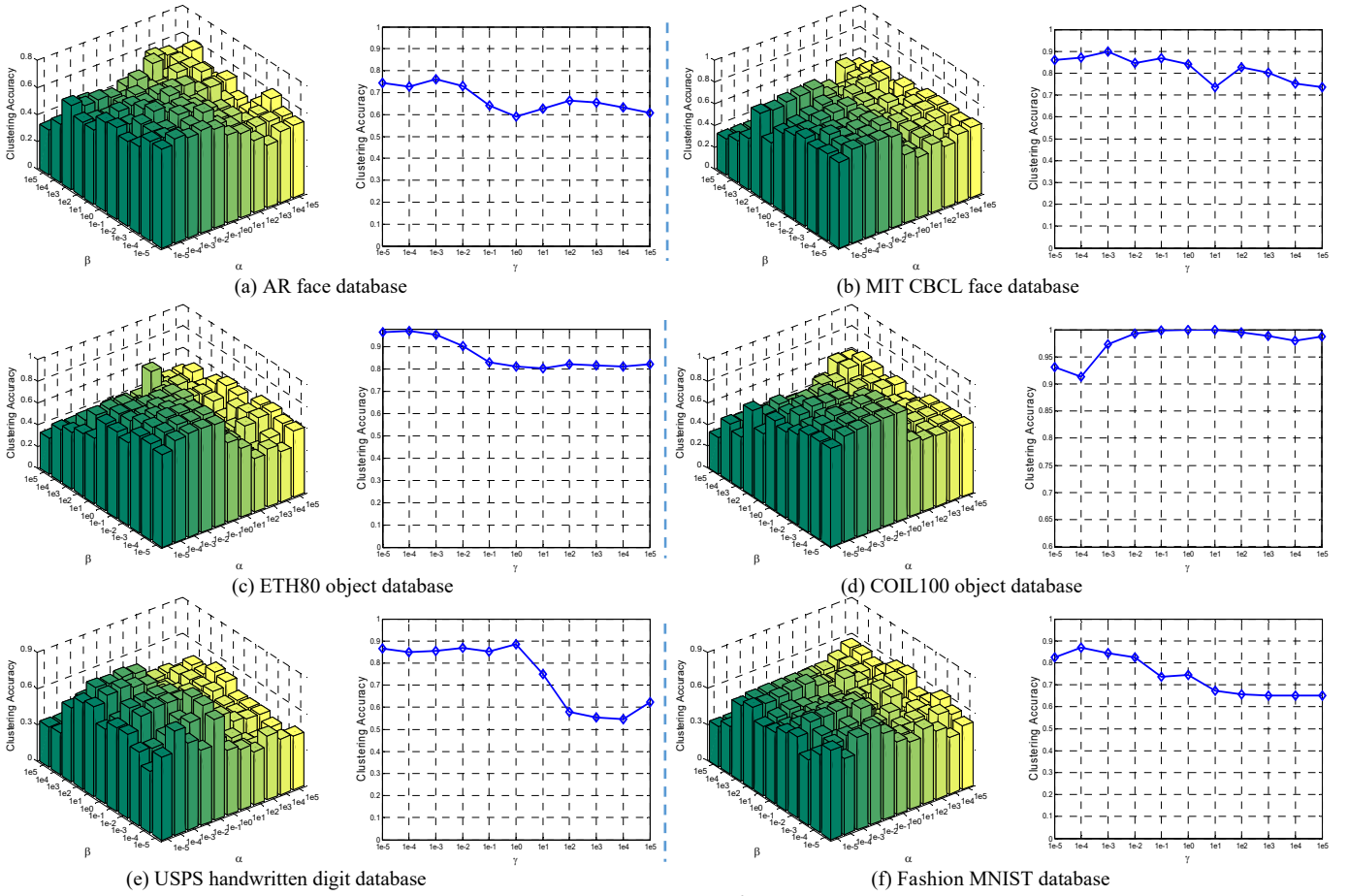


Figure 15: Clustering accuracies vs. varied parameters of our DS²CF-Net method based on the used databases.

Table 4: Parameter settings of our DS²CF-Net on used databases.

Database	α	β	γ
AR	10^{-1}	10^{-4}	10^{-3}
MIT CBCL	10^{-1}	10^{-4}	10^{-3}
ETH80	10^{-3}	10^{-4}	10^{-4}
COIL100	10^0	10^{-5}	10^1
USPS	10^{-1}	10^{-3}	10^0
Fashion MNIST	10^{-1}	10^{-3}	10^{-4}

VI. CONCLUDING REMARKS

We proposed a new enriched prior based dual-constrained deep semi-supervised coupled factorization network. Our model can discover deep hierarchical feature information, learning with a small number of labeled data and a large amount of unlabeled data. To mine hidden deep information, our DS²CF-Net designs a coupled hierarchical deep-structure and geometrical structure-constrained factorization network using multiple layers of linear transformations of basis vectors and representations. To improve the discriminating ability of learned deep representation and coefficients, DS²CF-Net clearly considers enriching the supervised prior by the joint deep coefficients-regularized label prediction, and incorporates enriched prior information as additional label and structure constraints. Moreover, DS²CF-Net also proposes to preserve the locality structures in both data space and feature space by adopting an adaptive dual-graph weighting strategy.

We have evaluated our DS²CF-Net for image representation and clustering, and the results are compared with related single-

layer and multilayer models. Visual image analysis and quantitative clustering evaluation demonstrate the effectiveness of our model. In future, we will evaluate our network for other related areas. A more effective coupled factorization strategy will also be investigated. Additionally, we will explore how to integrate the factorization model with the deep convolutional neural network for handling the large-scale vision tasks.

ACKNOWLEDGMENTS

This work is partially supported by the National Natural Science Foundation of China (61672365, 61732008, 61725203, 61622305, 61871444 and 61806035), the Fundamental Research Funds for the Central Universities of China (JZ2019-HGPA0102), and the Project Funded by the Priority Academic Program Development of Jiangsu Higher Education Institutions. Zhao Zhang is the corresponding author.

REFERENCES

- [1] I. T. Jolliffe, "Principal Component Analysis," *Springer Berlin*, vol.87, no.100, pp.41-64, 1986.
- [2] G. H. Golub, and C. Reinsch, "Singular value decomposition and least squares solutions," *Numerische mathematik*, vol.14, no.5, pp. 403-420, 1970.
- [3] R. Gray, "Vector quantization," *IEEE Assp Magazine*, vol.1, no.2, pp.4-29, 1984.
- [4] D. Lee, H. Seung, "Learning the parts of objects by non-negative matrix factorization," *Nature*, vol.401, pp. 788-791, 1999.

- [5] X. Wei and Y. Gong, "Document clustering by concept factorization," In: *Proceedings of the ACM SIGIR*, 2004.
- [6] D. Cai, X. F. He, J. Han, and T. Huang, "Graph regularized nonnegative matrix factorization for data representation," *IEEE Trans. Pattern Anal. Mach. Intell.*, vol.33, no.8, pp.1548-1560, 2011.
- [7] D. Cai, X. He and J. Han, "Locally consistent concept factorization for document clustering," *IEEE Transactions on Knowledge and Data Engineering*, vol.23, no.6, pp.902-913, 2011.
- [8] J. Ye, Z. Jin, "Graph-Regularized Local Coordinate Concept Factorization for Image Representation," *Neural Processing Letters*, vol.46, no.2, pp.427-449, 2017.
- [9] H. Li, J. Zhang, and J. Liu, "Graph-regularized CF with local coordinate for image representation," *Journal of Visual Communication & Image Representation*, vol.49, pp.392-400, 2017.
- [10] L. Dhillon, "Co-clustering documents and words using bipartite spectral graph partitioning," In: *Proceedings of the 17th ACM SIGKDD*, pp.269-274, 2001.
- [11] Q. Gu, J. Zhou, "Co-clustering on manifolds," In: *Proceedings of the 15th ACM SIGKDD*, pp.359-368, 2009.
- [12] F. Shang, L. Jiao and F. Wang, "Graph dual regularization non-negative matrix factorization for co-clustering," *Pattern Recognition*, vol.45, no.6, pp.2237-2250, 2012.
- [13] J. Ye, Z. Jin, "Dual-graph regularized concept factorization for clustering," *Neurocomputing*, vol.138, no.11, pp.120-130, 2014.
- [14] S. Roweis, and L. Saul, "Nonlinear dimensionality reduction by locally linear embedding," *Science*, vol.290, pp.2323- 2326, 2000.
- [15] J. Tenenbaum, V. de Silva, J. Langford, "A global geometric framework for nonlinear dimensionality reduction," *Science*, vol.290, no.5500, pp.2319-2323, 2000.
- [16] H. Liu, Z. Wu, and X. Li, "Constrained nonnegative matrix factorization for image representation," *IEEE Trans. on Pattern Anal. Mach. Intell.*, vol.34, no.7, pp.1299-1311, 2012.
- [17] H. Liu, G. Yang, and Z. Wu, "Constrained concept factorization for image representation," *IEEE Trans. on Cybernetics*, vol. 44, no.7, pp.1214-1224, 2014.
- [18] A. Cichocki, R. Zdunek, "Multilayer nonnegative matrix factorization," *Electron. Lett.*, vol.42, no.16, pp.947-948, Aug, 2006.
- [19] X. Li, C. X. Zhao, Z. Q. Shu, Q. Wang, "Multilayer Concept Factorization for Data Representation," In: *Proceedings of International Conference on Computer Science and Education*, Cambridge, UK, pp.486-491, 2015.
- [20] R. Rajabi, and H. Ghassemian, "Spectral Unmixing of Hyperspectral Imagery Using Multilayer NMF," *IEEE Geoscience and Remote Sensing Letters*, vol.12, no.1, pp.38-42, 2015.
- [21] X. Li, X. Shen, Z. Shu, Q. Ye, C. Zhao, "Graph regularized multilayer concept factorization for data representation," *Neurocomputing*, vol. 238, pp. 139-151, 2017.
- [22] Z. Li and J. Tang, "Weakly-supervised Deep Matrix Factorization for Social Image Understanding," *IEEE Transactions on Image Processing*, 1-1, vol.26, no.1, pp.276-288, 2017.
- [23] G. Trigeorgis, K. Bousmalis, S. Zafeiriou, and B. W. Schuller, "A deep matrix factorization method for learning attribute representations," *IEEE Trans. on Pattern Anal. Mach. Intell.*, vol. 39, no. 3, pp. 417-429, 2015.
- [24] S. H. Ma, L. F. Zhang, W. B. Hu, Y. P. Zhang, J. Wu and X. L. Li, "Self-Representative Manifold Concept Factorization with Adaptive Neighbors for Clustering," In: *Proceedings of the International Joint Conference on Artificial Intelligence*, Stockholm, Sweden, pp.2539-2545, July 2018.
- [25] J. Bergstra, D. Yamins, and D. Cox, "Making a Science of Model Search: Hyperparameter Optimization in Hundreds of Dimensions for Vision Architectures," In: *Proceedings of International Conference on Machine Learning*, Atlanta, USA, vol.28, no.1, pp.115-123, June 2013.
- [26] B. Weyrauch, J. Huang, B. Heisele, and V. Blanz, "Component based Face Recognition with 3D Morphable Models," In: *Proceedings of the IEEE Workshop on Face Processing in Video*, Washington, D.C., 2004.
- [27] S Nayar, S Nene, H Murase, "Columbia object image library (coil 100)," *Department of Comp. Science, Columbia University, Tech. Rep. CUCS-006-96*, 1996.
- [28] B. Leibe, B. Schiele, "Analyzing appearance and contour based methods for object categorization," In: *Proceedings of the IEEE Conference on Computer Vision and Pattern Recognition*, pp.409-415, 2003.
- [29] J. Hull, "A database for handwritten text recognition research," *IEEE Trans. on Pattern Anal. Mach. Intell.*, vol.16, no.5, pp.550-554, 1994.
- [30] Z. He, S. Yi, Y.M. Cheung, X. You, and Y.Y. Tang, "Robust object tracking via key patch sparse representation," *IEEE Transactions on Cybernetics*, vol.47, no.2, pp.354-364, 2017.
- [31] J. Yang, and J. Yang, "From image vector to matrix: a straight forward image projection technique—IMPCA vs. PCA," *Pattern Recognition*, vol.35, no.9, pp.1997-1999, 2002.
- [32] Z. Zhang, F. Li, and M. Zhao, L. Zhang and S. Yan, "Joint Low-Rank and Sparse Principal Feature Coding for Enhanced Robust Representation and Visual Classification," *IEEE Trans. on Image Processing*, vol.25, no.6, pp.2429-2443, 2016.
- [33] J. Ren, Z. Zhang, S. Li, Y. Wang, G. Liu, S. Yan and M. Wang, "Learning Hybrid Representation by Robust Dictionary Learning in Factorized Compressed Space," *IEEE Transactions on Image Processing*, Dec 2019.
- [34] M. Sugiyama, "Dimensionality reduction of multimodal labeled data by local fisher discriminant analysis," *Journal of Machine Learning Research*, vol.8, pp.1027-1061, 2007.
- [35] D. Cai, X. He, J. Han, "Document clustering using locality preserving indexing," *IEEE Transactions on Knowledge and Data Engineering*, vol.17, no.12, pp.1624-1637, 2005.
- [36] X. He, D. Cai and P. Niyogi, "Laplacian score for feature selection," *Advances in neural information processing systems*, 2006.
- [37] L. Lovasz, M. Plummer, "Matching Theory," *North Holland*, Budapest: Akadémiai Kiadó, 1986.
- [38] Y. Yang, H. Shen, Z. Ma, Z. Huang, X. Zhou, "L2, 1-Norm Regularized Discriminative Feature Selection for Unsupervised Learning," In: *Proceedings of IJCAI*, Barcelona, Spain, 2011.
- [39] C. Hou, F. Nie, X. Li, D.Y. Yi, and Y. Wu, "Joint Embedding Learning and Sparse Regression: A Framework for Unsupervised Feature Selection," *IEEE Trans. Cybernetics*, vol.44, no.6, pp.793-804, 2014.
- [40] Z. Zhang, Y. Zhang, S. Li, G. Liu, D. Zeng, S. Yan, and M. Wang, "Flexible Auto-weighted Local-coordinate Concept Factorization: A Robust Framework for Unsupervised Clustering," *IEEE Trans. on Knowledge and Data Engineering*, Sep 2019.
- [41] Z. Zhang, Y. Zhang, S. Li, G. Liu, M. Wang, and S. Yan, "Robust Unsupervised Flexible Auto-weighted Local-Coordinate Concept Factorization for Image Clustering," In: *Proceedings of IEEE ICASSP*, Brighton, UK, pp.2092-2096, May 2019.
- [42] Z. Zhang, Y. Zhang, G. Liu, J. Tang, S. Yan and M. Wang, "Joint Label Prediction based Semi-Supervised Adaptive Concept Factorization for Robust Data Representation," *IEEE Transactions on Knowledge and Data Engineering*, Jan 2019.
- [43] Y. Zhang, Z. Zhang, Z. Zhang, M. Zhao, L. Zhang, Z. Zha and M. Wang, "Deep Self-representative Concept Factorization Network for Representation Learning," In: *Proceedings of SDM*, Cincinnati, USA, 2019.
- [44] X. Li, G. Cui, and Y. Dong, "Graph Regularized Non-Negative Low-Rank Matrix Factorization for Image Clustering," *IEEE Trans. on Cybernetics*, vol.47, no.11, pp.3840-3853, 2017.
- [45] R. Zhao, V. Tan, "A Unified Convergence Analysis of the Multiplicative Update Algorithm for Regularized Nonnegative Matrix Factorization," *IEEE Trans. Signal Processing*, vol. 66, no.1, pp.129-138, 2018.
- [46] H. Xiao, K. Rasul, R. Vollgraf, "Fashion-mnist: a novel image dataset for benchmarking machine learning algorithms," *arXiv: 1708.07747v2*, 2017.
- [47] M. Belkin, P. Niyogi, "Laplacian eigenmaps for dimensionality reduction and data representation," *Neural Computation*, vol.15, no.6, pp. 1373-1396, 2003.
- [48] Y. Peng, R. X. Tang, W. Z. Kong, J. H. Zhang, F. P. Nie and A. Cichocki, "Joint Structured Graph Learning and Clustering Based on Concept Factorization," In: *IEEE ICASSP*, Brighton, UK, pp. 3162-3166, 2019.
- [49] X. K. Ma, D. Dong, and Q. Wang, "Community Detection in Multi-Layer Networks Using Joint Nonnegative Matrix Factorization," *IEEE Trans. on Knowledge and Data Engineering*, vol.31, no.2, pp.273-286, 2019.
- [50] T. Xiao, H. Tian, and H. Shen, "Variational Deep Collaborative Matrix Factorization for Social Recommendation," In: *Proceedings of PAKDD*, Macau, China, pp.426-437, April 2019.
- [51] B. H. Lin, X. M. Tao, and J. H. Lu, "Hyperspectral Image Denoising via Matrix Factorization and Deep Prior Regularization," *IEEE Transactions on Image Processing*, vol.29, pp. 565-578, 2020.